Edinburgh Research Explorer

Development of a high-speed line-scanning FLIM microscope for biological imaging

Development of a high-speed line-scanning FLIM microscope for biological imaging

HANNING MAI[2,3], ANNELIESE JARMAN[1], AHMET T. ERDOGAN[2], CONOR TREACY[1,4], NEIL FINLAYSON[2], ROBERT K. HENDERSON[2] AND SIMON P. POLAND[1,*]

[1]*Comphrehensive Cancer Centre, School of Cancer and Pharmaceutical Sciences, King's College London, UK.*
[2]*Institute for Integrated Micro and Nano Systems, University of Edinburgh, Edinburgh, UK*
[3]*Now at Sony Europe Technology Development Centre, 38123 Trento, Italy.*
[4]*Now at the Wellcome Centre for Cell Biology, School of Biological Sciences, University of Edinburgh, Edinburgh, UK*

Corresponding author: simon.poland@kcl.ac.uk

We report the development of a novel line-scanning microscope capable of acquiring high-speed TCSPC-based FLIM. The system consists of a laser-line focus, which is optically conjugated to a 1024 × 8 single photon avalanche diode (SPAD) based line-imaging CMOS, with 23.78 μm pixel pitch at 49.31% fill factor. Incorporation of on-chip histogramming on the line-sensor enables acquisition rates 33 times faster than our previously reported bespoke high speed FLIM platforms. We demonstrate the imaging capability of the high-speed FLIM platform in a number of biological applications.

For fluorescence lifetime imaging microscopy (FLIM), time-correlated single photon counting (TCSPC) is unparalleled in its measurement accuracy particularly for multi-exponential decays [1, 2]. Until recently, high speed FLIM could only be performed using modulated or time-gated image intensifier systems [3, 4] as TCSPC was fundamentally limited with respect to photon counting rate in implementations of laser scanning microscopy [1]. This has restricted its use in several time-critical applications including in-vivo imaging, diagnostics, and histological screening.

One of the main issues limiting single photon acquisition speeds in conventional TCSPC was the long period, known as electronic dead time, between which the system could measure consecutive photon measurements. This has restricted the maximum photon rate to no more than 5% or less than the repetition rate of the laser in order to avoid pulse pile up and distortion of the fluorescence lifetime readout [5, 6]. Recently the incorporation of improved time-to-digital convertor (TDC) electronics has dramatically reduced the dead time between consecutive pulses and facilitated count rates up to 80 Mega-photon counts/s [7, 8]. New FLIM platforms have also been presented utilizing time-gated SPAD arrays for widefield imaging [9] and fast digitization approaches to perform direct pulse sampling [10, 11]. Whilst extremely fast, facilitating image frame rate acquisitions up to 1 kHz with spatial binning [12], the performance of these fast digitization systems is compromised by the relatively long system instrument response functions (IRFs) (>1 ns), which makes it difficult to detect lower fluorescence lifetimes and reduces the temporal resolution of the measured fluorescence lifetime decays [13].

Recently we have shown multifocal fluorescence lifetime imaging microscopy (M-FLIM) for confocal and multiphoton applications utilizing TCSPC [14-16] which dramatically increases the acquisition rate of high-resolution fluorescence lifetime imaging by parallelizing excitation and detection. Parallelized detection with TCSPC was achieved using specialized 32 x 32 10-bit TDC array (~55 ps) each with their own integrated low dark-count single-photon avalanche diodes (SPAD).

In this Letter, we report the development of a novel line-scanning microscope capable of acquiring high-speed TCSPC-based fluorescence lifetime images. The system consists of a laser-line focus, which is optically conjugated to a 1024 × 8 SPAD based line imaging CMOS, with 23.78 μm pixel pitch and 49.31% fill factor [17]. Utilising a cylindrical lens to generate a laterally stretched Gaussian intensity distribution beam and incorporation of a single galvanometer scanner with relay optics, we have been able to simplify the optical footprint of the system. The incorporation of on-chip histogramming directly on the CMOS line-sensor electronics enables acquisition rates 33 times faster [15] than our previously reported bespoke high speed FLIM platforms.

To evaluate the performance and high-speed capabilities of the FLIM system we demonstrate its use in imaging several biologically relevant samples. Whilst this CMOS line-sensor has previously been incorporated into a point scanning confocal setup [18], this is the first time that it has been used in a line-scanning FLIM.
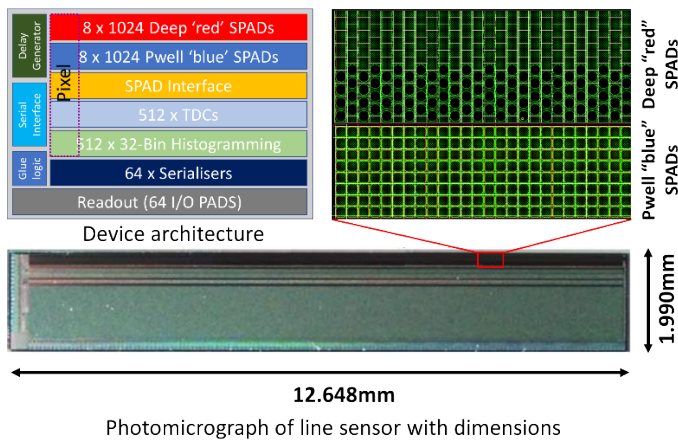
Fig. 1. Showing the line sensor block diagram, individual pixel architecture and alignment and line sensor device dimensions.

A simplified diagram of the linear device [17, 19] architecture is shown in Fig 1. The sensor measuring 12.628 mm × 1.990 mm is fabricated by a 130 nm CMOS technology process. The device is composed of two individual sets of 1024 × 8 SPAD detectors, optimized to blue (450nm – 550nm) and red (600nm – 900nm) spectral regions respectively. Full characterization of this chip set and comparison with other existing technologies has already been presented elsewhere [17, 19]. For this paper only the blue sensitive SPAD arrays are used, which have an average IRF of 162 ps, median dark count rate (DCR) of 400 Hz and photo detection probability (PDP) of 40% @ 480 nm [17]. The SPAD array is split into 512 individual 'pixels', where each pixel is composed of 2 × 8 SPAD sub-arrays, all of which can be independently addressed and activated to provide customized structured detection. Each individual pixel has its own dedicated 16-bit TDC and can be operated in either conventional TCSPC mode or in on-chip histogramming mode, whereby individual photon arrival times for each pixel can be passed into and stored in their respective bin block. These histograms are then read off the chip after an externally triggered event. In histogramming mode, the bin width can be configured from 51.2 ps to 6.55 ns providing a window range from 1.64 ns to 209.92 ns [17]. The linear array sensor and PCB interfaces with the computer via an FPGA circuit board (Opal Kelly, XEM6310).

The line-scanning optical layout is shown in Fig. 2. The system has been built around a Nikon Eclipse Ti inverted microscope for stability and ease of sample mounting. Laser light from a Ti:Sapphire laser system (Coherent, Chameleon Ultra II) is frequency-doubled using LBO non-linear crystal to generate 490 nm output and then expanded with lenses L1 and L2 onto a cylindrical lens CL (Thorlabs, LJ1567L2, f = 100 mm) to generate the line beam. This is then imaged through a dichroic filter (Semrock, FF509-Di01) onto a single-axis scanning mirror (Thorlabs, GVS011/M). The line beam is then directed through a scan lens SL (Thorlabs, AC254-100-A-ML, f=100 mm) and tube lens (f = 200 mm) onto the back pupil of a x40 0.75 N.A. air objective lens OL (Nikon Instruments Ltd.). The horizontal line beam at the horizontally scanning mirror is conjugate to the back pupil of the objective to facilitate a sweeping line-scan directly on the sample plane. Fluorescence is collected by the same objective lens, relayed, de-scanned and then reprojected onto the blue sensitive portion of linear array sensor with the dichroic and lens L3 (Thorlabs AC254-200-A-ML, f = 200 mm). The beamlet magnification is chosen to

align the fluorescence line image at the correct orientation with respect to the detector array and utilizes the full 512 pixels of the detector array.
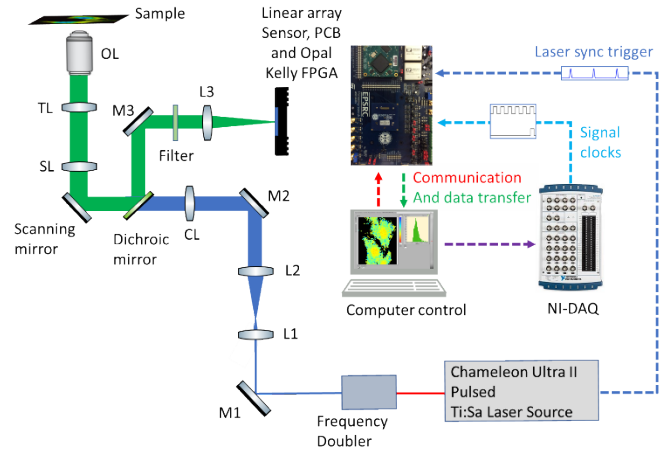

Fig. 2. Simplified view of the confocal line-scanning FLIM system, outlining the optical set up and computer control.

To acquire an image, signals are generated from a high-speed data acquisition device (National Instruments, Ni-DAQ, USB-6363) to synchronize the scanning galvanometer position with the data acquisition from the linear sensor. For each scanning step (driven using a ramping voltage applied to the galvanometer), the linear sensor array acquires photon arrival times to generate a 32-bin histogram for each pixel. At the end of the exposure cycle, 512 histograms are sent to the computer via a USB3.0 bus. The line sweeps across the sample and the light collected is reconstructed into a 512 x 512 x 32 data set. All aspects of the microscope system are controlled using custom-developed software written in LabVIEW. The system can be operated to perform an acquisition at a single plane or at multiple depths to generate a 3-dimensional image.

To illustrate and evaluate the capabilities of the imaging platform to obtain FLIM datasets, images of Convallaria Majalis (Lily of the valley) were acquired (Fig. 3). Datasets were acquired at 490 nm excitation in 500 ms and fluorescence lifetimes for each pixel determined from their corresponding transient decays. The typical beam input power ~1-2 mW has been applied at the cylindrical lens to generate the laser line focus. For the data presented here lifetimes were calculated using a differential centre-of-mass method (CMMdiff) [16] for real-time readout. As the histogram data has been generated and saved, lifetime calculations could also be performed offline using Levenberg–Marquardt fitting to provide more accurate determination. As each pixel on the sensor has its own TDC, limitations in the fabrication process gives rise to distinct characteristics, resulting in a variability in the start point for each histogram. In order to compensate for this, precise positioning of the start point for each TDC was determined using the CMM from IRF measurements and then offsets applied off-chip to correct the lifetime readouts.
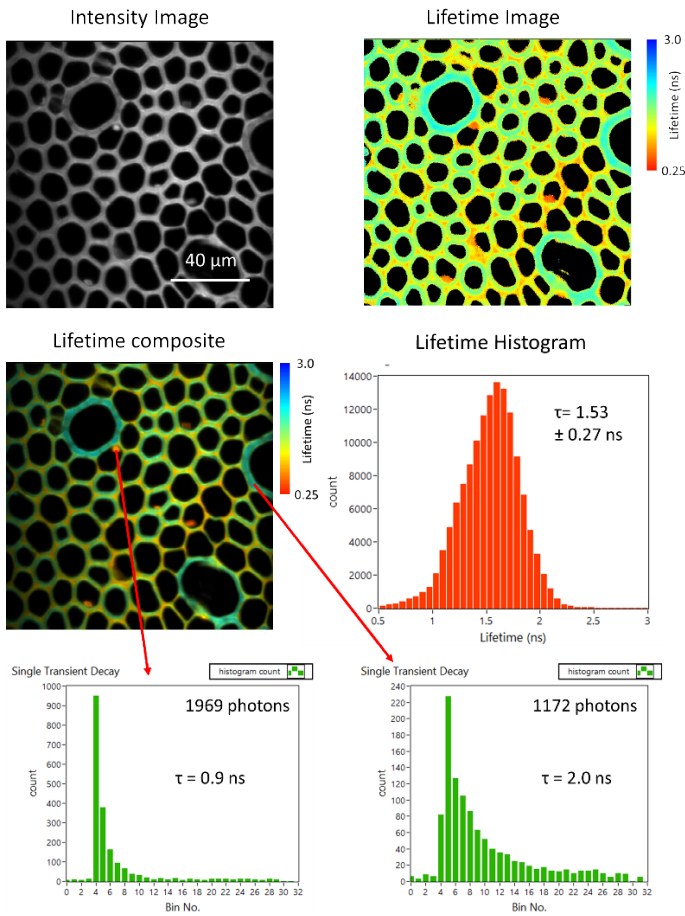
Fig. 3. Convallaria Majalis dataset acquired in 500 ms. Intensity, lifetime and intensity weighted lifetime composite images are presented. Image size 512 (135 μm) × 512 (135 μm). A histogram of the lifetime distribution and raw transient decays of individual example pixels are also presented.

As mentioned previously, the line detector array [19, 20] has been shown to have a variable temporal window which can be adjusted by the user. For this set-up the temporal window was adjusted to 13.11 ns, with a temporal bin size of 409.6 ps, to closely match the pulsed laser modulation of 80 MHz. To demonstrate the capability of the system to provide intensity and FLIM images of high dynamic range at high-speed, we imaged mouse pulmonary tissue sample stained with hematoxylin and eosin (H&E) provided by Calamat Ltd. In Fig. 4 datasets were taken of two example regions of the sample and the intensity and lifetime histograms presented. For a 512 × 512 image this translates as many 1000s of photons/pixel/s (as shown in the intensity histograms), negating the need to perform spatial pixel-binning to provide accurate lifetime determinations.

The incorporation of a motorized stage (Ti-S-ER) on the Nikon Ti microscope enables positional control of the sample and facilitates the high-speed acquisition of tiled mosaic FLIM images. Due to the high-speed imaging capability of the system, these macroscale datasets can be acquired in the order of seconds, whilst still providing FLIM information and diffraction limited resolution. In Fig. 5 examples of this mosaic functionality are shown. To generate a 2 mm × 2 mm mosaic in 49 seconds, 14 × 14 (196) images were acquired at acquisition times of 250 ms. The Mouse

Lung H&E macro image was acquired in 12.5 seconds and composed of 7 × 7 individual images.

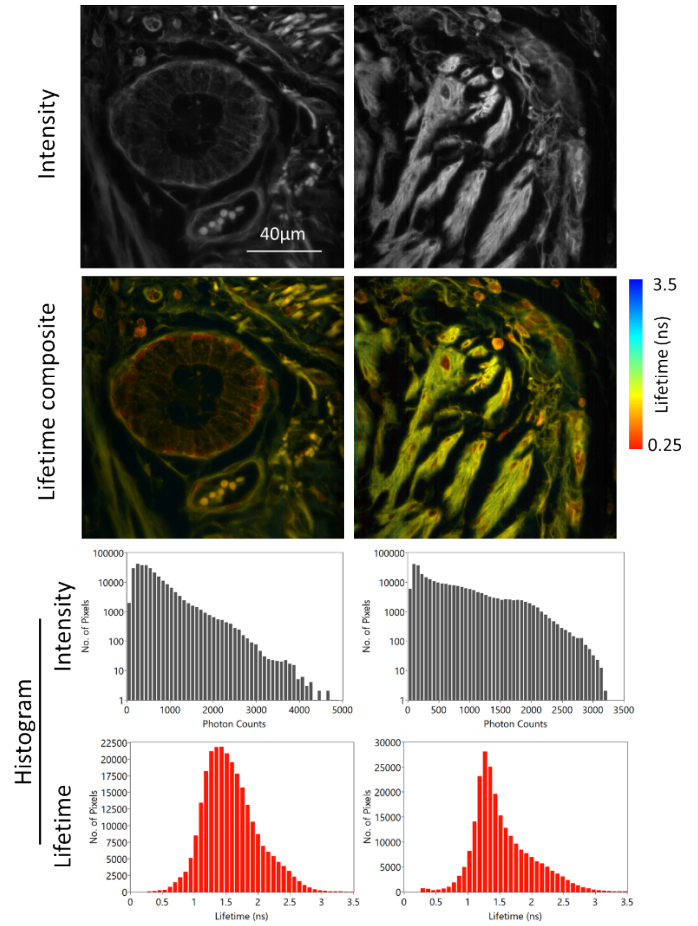**Fig. 4.** Single intensity and lifetime composite images of mouse pulmonary sample stained with H& E. Image size 512 (135 μm) x 512 (135 μm). Total image acquisition time = 500 ms. Intensity and lifetime histograms of each dataset are also displayed.
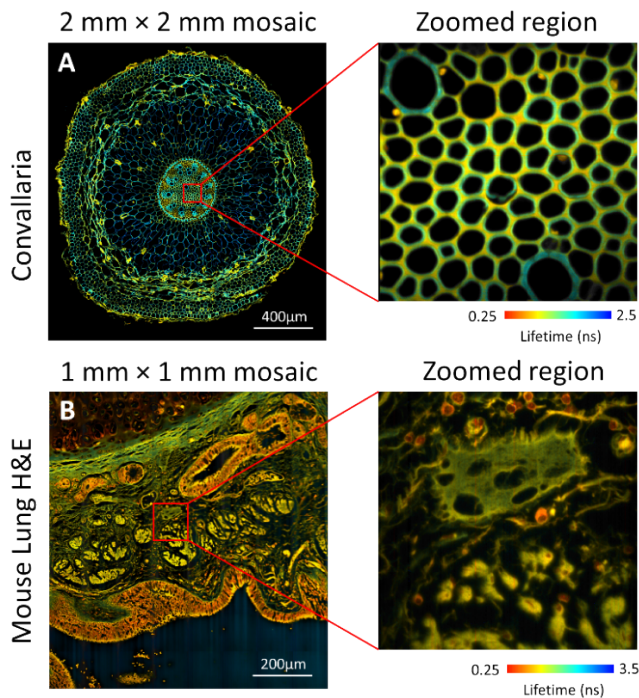
Fig. 5. Macroscale FLIM composite images of **A** Convallaria Majalis (7168 × 7168 pixels) acquired in 49 seconds and **B** Mouse Lung H&E sample (3584 × 3584 pixels) acquired in 12.5 seconds. Zoomed regions of single image tiles (512 × 512) are also included.

In summary, we have developed a high-speed line scanning FLIM microscope for biological imaging applications. We have demonstrated that line generation and laser-line scanning in conjunction with on-chip histogramming on a linear SPAD array sensor is practical, fast and offers novel advantages for fluorescence lifetime imaging. We have presented the system operating at acquisition speeds up to 4 frames/s, acquiring many thousands of photons per second per pixel without the need to perform pixel binning. Whilst the maximum photon counting rates of this device has been quoted previously as 16.5 GHz [17], this is only achievable in strong light conditions where the sample imaged is homogeneous in intensity. In most cases we would expect the sample imaged to be highly heterogeneous in nature and this maximum count rate would not be achieved. Each of the 512 pixels on the line sensor is capable of simultaneously acquiring a maximum of 32.23 Mega-photon counts/s, facilitating high speed parallelized image acquisition.

For samples with low levels of fluorescence, the mass-parallelization of both fluorescent excitation and detection provides a great advantage over single beam scanning FLIM technologies, where the high laser power excitation required at short pixel dwell times for high-speed FLIM acquisition will undoubtedly perturb or damage the sample. For the images presented here the system was operating much less than 1% of the total laser output power. This provides us with the dynamic range required to acquire datasets for photon starved samples and applications. In future, with further improvements to control software and FPGA firmware should enable acquisition speeds up to 30 frames/s.

References

1. E. Gratton, S. Breusegem, J. Sutin, Q. Ruan, and N. Barry, Journal of biomedical optics **8**, 381-390 (2003).
2. A. Esposito, H. C. Gerritsen, and F. S. Wouters, JOSA A **24**, 3261-3273 (2007).
3. D. M. Grant, J. McGinty, E. McGhee, T. Bunney, D. Owen, C. Talbot, W. Zhang, S. Kumar, I. Munro, and P. Lanigan, Optics express **15**, 15656-15673 (2007).
4. T. Omer, L. Zhao, X. Intes, and J. Hahn, Journal of biomedical optics **19**, 086023-086023 (2014).
5. H. C. Gerritsen, A. Agronskaia, A. Bader, and A. Esposito, Laboratory Techniques in Biochemistry and Molecular Biology **33**, 95-132 (2009).
6. X. Liu, D. Lin, W. Becker, J. Niu, B. Yu, L. Liu, and J. Qu, Journal of Innovative Optical Health Sciences **12**, 1930003 (2019).
7. M. Koenig, S. Orthaus-Mueller, R. Dowler, B. Kraemer, A. Tannert, O. Schulz, T. Roehlicke, M. Wahl, H.-J. Rahn, and M. Patting, Biophysical Journal **112**, 298a (2017).
8. M. Loidolt-Krüger, F. Jolmes, M. Patting, M. Wahl, E. Sisamakis, and R. Erdmann, Time-correlated single photon counting—the underlying technology Overcoming challenges of TCSPC at high count rates, 1-8 (2021).
9. A. Ulku, A. Ardelean, M. Antolovic, S. Weiss, E. Charbon, C. Bruschini, and X. Michalet, Methods and applications in fluorescence **8**, 024002 (2020).
10. M. Eibl, S. Karpf, D. Weng, H. Hakert, T. Pfeiffer, J. P. Kolb, and R. Huber, Biomedical optics express **8**, 3132-3142 (2017).
11. X. Y. Dow, S. Z. Sullivan, R. D. Muir, and G. J. Simpson, Optics letters **40**, 3296-3299 (2015).
12. S. Karpf, C. T. Riche, D. Di Carlo, A. Goel, W. A. Zeiger, A. Suresh, C. Portera-Cailliau, and B. Jalali, Nature communications **11**, 1-9 (2020).
13. J. E. Sorrells, R. R. Iyer, L. Yang, E. J. Chaney, M. Marjanovic, H. Tu, and S. A. Boppart, Optics Express **29**, 37759-37775 (2021).
14. S. P. Poland, N. Krstajić, J. Monypenny, S. Coelho, D. Tyndall, R. J. Walker, V. Devauges, J. Richardson, N. Dutton, and P. Barber, Biomedical optics express **6**, 277-296 (2015).
15. N. Krstajić, S. Poland, J. Levitt, R. Walker, A. Erdogan, S. Ameer-Beg, and R. K. Henderson, Optics letters **40**, 4305-4308 (2015).
16. S. P. Poland, A. T. Erdogan, N. Krstajić, J. Levitt, V. Devauges, R. J. Walker, D. D.-U. Li, S. M. Ameer-Beg, and R. K. Henderson, Optics express **24**, 6899-6915 (2016).
17. A. T. Erdogan, R. Walker, N. Finlayson, N. Krstajić, G. Williams, J. Girkin, and R. Henderson, IEEE Journal of Solid-State Circuits **54**, 1705-1719 (2019).
18. G. O. Williams, E. Williams, N. Finlayson, A. T. Erdogan, Q. Wang, S. Fernandes, A. R. Akram, K. Dhaliwal, R. K. Henderson, and J. M. Girkin, Nature communications **12**, 1-9 (2021).
19. A. T. Erdogan, R. Walker, N. Finlayson, N. Krstajic, G. O. Williams, and R. K. Henderson, "A 16.5 giga events/s 1024× 8 spad line sensor with per-pixel zoomable 50ps-6.4 ns/bin histogramming tdc," in *2017 Symposium on VLSI Circuits*(IEEE2017), pp. C292-C293.
20. A. T. Erdogan, N. Finlayson, G. O. Williams, E. Williams, and R. K. Henderson, "Video rate spectral fluorescence lifetime imaging with a 512 x 16 spad line sensor," in *High-Speed Biomedical Imaging and Spectroscopy IV*(SPIE2019), pp. 15-24.

References with paper titles for review

1. Gratton E, Breusegem S, Sutin J, Ruan Q, Barry N. Fluorescence lifetime imaging for the two-photon microscope: time-domain and frequency-domain methods. Journal of biomedical optics. 2003;8(3):381-90.

2. Esposito A, Gerritsen HC, Wouters FS. Optimizing frequency-domain fluorescence lifetime sensing for high-throughput applications: photon economy and acquisition speed. JOSA A. 2007;24(10):3261-73.

3. Grant DM, McGinty J, McGhee E, Bunney T, Owen D, Talbot C, et al. High speed optically sectioned fluorescence lifetime imaging permits study of live cell signaling events. Optics express. 2007;15(24):15656-73.

4. Omer T, Zhao L, Intes X, Hahn J. Reduced temporal sampling effect on accuracy of time-domain fluorescence lifetime Förster resonance energy transfer. Journal of biomedical optics. 2014;19(8):086023-.

5. Gerritsen HC, Agronskaia A, Bader A, Esposito A. Time domain FLIM: theory, instrumentation, and data analysis. Laboratory Techniques in Biochemistry and Molecular Biology. 2009;33:95-132.

6. Liu X, Lin D, Becker W, Niu J, Yu B, Liu L, et al. Fast fluorescence lifetime imaging techniques: A review on challenge and development. Journal of Innovative Optical Health Sciences. 2019;12(05):1930003.

7. Koenig M, Orthaus-Mueller S, Dowler R, Kraemer B, Tannert A, Schulz O, et al. Rapid Flim: The New and Innovative Method for Ultra-Fast Imaging of Biological Processes. Biophysical Journal. 2017;112(3):298a.

8. Loidolt-Krüger M, Jolmes F, Patting M, Wahl M, Sisamakis E, Erdmann R. Visualize dynamic processes with rapidFLIM HiRes, the ultra fast FLIM imaging method with outstanding 10 ps time resolution. Time-correlated single photon counting–the underlying technology Overcoming challenges of TCSPC at high count rates. 2021:1-8.

9. A. Ulku, A. Ardelean, M. Antolovic, S. Weiss, E. Charbon, C. Bruschini, and X. Michalet, Methods and applications in fluorescence **8**, 024002 (2020).

10. Eibl M, Karpf S, Weng D, Hakert H, Pfeiffer T, Kolb JP, et al. Single pulse two photon fluorescence lifetime imaging (SP-FLIM) with MHz pixel rate. Biomedical optics express. 2017;8(7):3132-42.

11. Dow XY, Sullivan SZ, Muir RD, Simpson GJ. Video-rate two-photon excited fluorescence lifetime imaging system with interleaved digitization. Optics letters. 2015;40(14):3296-9.

12. Karpf S, Riche CT, Di Carlo D, Goel A, Zeiger WA, Suresh A, et al. Spectro-temporal encoded multiphoton microscopy and fluorescence lifetime imaging at kilohertz frame-rates. Nature communications. 2020;11(1):1-9.

13. Sorrells JE, Iyer RR, Yang L, Chaney EJ, Marjanovic M, Tu H, et al. Single-photon peak event detection (SPEED): a computational method for fast photon counting in fluorescence lifetime imaging microscopy. Optics Express. 2021;29(23):37759-75.

14. Poland SP, Krstajić N, Monypenny J, Coelho S, Tyndall D, Walker RJ, et al. A high speed multifocal multiphoton fluorescence lifetime imaging microscope for live-cell FRET imaging. Biomedical optics express. 2015;6(2):277-96.

15. Krstajić N, Poland S, Levitt J, Walker R, Erdogan A, Ameer-Beg S, et al. 0.5 billion events per second time correlated single photon counting using CMOS SPAD arrays. Optics letters. 2015;40(18):4305-8.

16. Poland SP, Erdogan AT, Krstajić N, Levitt J, Devauges V, Walker RJ, et al. New high-speed centre of mass method incorporating background subtraction for accurate determination of fluorescence lifetime. Optics express. 2016;24(7):6899-915.

17. Erdogan AT, Walker R, Finlayson N, Krstajić N, Williams G, Girkin J, et al. A CMOS SPAD line sensor with per-pixel histogramming TDC for time-resolved multispectral imaging. IEEE Journal of Solid-State Circuits. 2019;54(6):1705-19.

18. Williams GO, Williams E, Finlayson N, Erdogan AT, Wang Q, Fernandes S, et al. Full spectrum fluorescence lifetime imaging with 0.5 nm spectral and 50 ps temporal resolution. Nature communications. 2021;12(1):1-9.

19. Erdogan AT, Walker R, Finlayson N, Krstajic N, Williams GO, Henderson RK, editors. A 16.5 Giga Events/s 1024× 8 SPAD Line Sensor with per-pixel Zoomable 50ps-6.4 ns/bin Histogramming TDC. 2017 Symposium on VLSI Circuits; 2017: IEEE.

20. Erdogan AT, Finlayson N, Williams GO, Williams E, Henderson RK, editors. Video rate spectral fluorescence lifetime imaging with a 512 x 16 SPAD line sensor. High-Speed Biomedical Imaging and Spectroscopy IV; 2019: SPIE.